Judith K. Maizels*

Aberdeen

FREQUENCY OF RELIC FROST-FISSURE STRUCTURES AND PREDICTION OF POLYGON PATTERN A QUANTITATIVE APPROACH

Abstract

The location of fifty relic frost fissures exposed in Devensian outwash deposits in a Scottish gravel pit were mapped, and the observed fissure distributions were compared with similar data obtained from transect measurements based on aerial photographs and published maps of frost-fissure polygonal networks in Europe and North America. These measurements provided a series of empirical, predictive equations relating the distributions of fissure structures exposed along linear transects to the areal pattern of associated polygonal networks, in turn allowing former polygon diameters and likely paleo-polygonal patterns to be predicted. Although some of the fissure structures appear to be of syngenetic origin, the majority are epigenetic and are believed to date from Younger Dryas times. Wedge frequency and predicted polygon diameters in the Scottish gravel pit compare closely with active ice-wedge polygons in Northern Alaska and Arctic Canada, suggesting that during Younger Dryas times permafrost was probably extensive and mean annual temperatures were up to 16°C lower in eastern Scotland than at present.

INTRODUCTION

Relic frost fissures have been observed in numerous parts of northern Europe and North America, particularly in Pleistocene fluvioglacial sands and gravels. The literature generally refers to their possible age, origin, and sedimentology, together with the stratigraphy of the sites. However, little analysis has been directed toward the local distribution of the fissure structures, the pattern, the density and the variability of their distribution. Few attempts, other than those by Goździk (1964, 1973), have determined whether the distribution of relic fissure structures is related to the distribution of any associated network of former frost-fissure or ice-wedge polygons. This paper aims to demonstrate that the distribution of fissure structures present along linear sections and exposures may be a valuable tool in the prediction of the likely size, density and pattern of associated paleo-polygonal networks, and hence in the interpretation of paleo-environmental conditions.

The development of an ice-wedge polygon network is believed to represent a response of a moisture-rich sediment body to rapid ground freezing in areas

* Department of Geography, University of Aberdeen, St. Mary's, High Street, Old Aberdeen, AB9 2UF, Scotland, U.K.

of permafrost; as large thermal stresses are generated in the surface sediments during freezing, contraction cracks develop, and the resulting fissures are periodically filled with water which then freezes and accumulates to form wedge ice. Ice-wedge polygons comprise three-dimensional networks of contraction cracks, filled with wedge ice, while frost-wedge polygons lack ice infill. However, polygon networks are highly variable in size, density and pattern, differences that may reflect variations in temperature conditions and moisture content of the sediment body. Polygon diameter, for example, may reflect the severity and/or the duration of permafrost conditions, such that larger polygons may develop under "milder" or less continuous permafrost conditions (e.g. LACHENBRUCH, 1962; DYLIK, 1966) or during a shorter period of time (e.g. ÖHRNGREN, 1967) since smaller, secondary polygons may have had less chance of developing. Other workers, however, (e.g. MORGAN, 1971), claim the reverse, suggesting that under less severe permafrost conditions moisture tensions are greater, and hence maximum ground cracking will occur, producing numerous smaller polygons. According to DOSTOVALOV and POPOV (1966) the frequency of ice-wedge occurrence and the spacing of polygons of different generations depend on the "sharpness of minimum temperatures" at the top of the permafrost. PÉWÉ (1966, 1973) demonstrates that active ice-wedge development in Alaska is confined to areas experiencing mean annual air temperatures less than $-6°$ to $-8°C$; however, the minimum ground temperatures required for ice-wedge polygons to develop depend on the texture of the sediment body. The limiting mean temperature requirements for ice-wedge formation in finer-grained sediments are only $-2°$ to $-3°C$ (ROMANOVSKIJ and ŠAPOŠNIKOVA, 1971, *in* GOŹDZIK, 1973), while in coarser-grained sediments minimum temperatures of less than $-7°$ to $-8°C$ are required although temperatures of $-15°$ to $-20°C$ may be necessary at the top of the permafrost (PÉWÉ, 1966). Hence polygon density is expected to be much higher in finer-grained sediments where conditions are more conducive to the movement of ground moisture. Moisture content also acts as an important control on polygon size since drier sediments have lower coefficients of expansion and possess smaller thermal strains (LACHENBRUCH, 1966), so giving rise to larger polygons.

The surface expression of these polygons has attracted much attention from geomorphologists since the polygon networks can often readily be detected and mapped from both aerial and ground surveys (e.g. RAPP and ANNERSTEN, 1969; FRIEDMAN, *et al.*, 1971; MORGAN, 1971; SVENSSON, 1972, 1973, 1976; WALTERS, 1978). Inspection of surface polygon networks indicates that they exhibit a wide variety of patterns, including those described as "orthogonal", "hexagonal", "random" or mixed arrangements of fissures and enclosed "cells". The observed geometric properties of polygon patterns represent a response of the contracting sediment body to the relative regularity of the internal thermal stresses that control the generation and propagation of fissures (LACHENBRUCH, 1966). Hence, the regularity or uniformity of a polygonal pattern must reflect the extrinsic and intrinsic factors that control the variability of thermal stresses within the sediment. Rates of freezing and the degree of freezing act as major extrinsic controls, while the intrinsic controls of the sediment body itself include sediment porosity, permeability and tensile strength, moisture content and ice content, sediment thickness and the nature of the underlying bedrock. Polygon size and pattern are thus largely controlled by the nature and duration of a particular air and ground temperature regime, by the contraction capacity of the sediment body, and by any pre-existing pattern of fissures and weaknesses. Many of the relationships between these environmental controls and the resulting polygon pattern, however, remain unclear. The present paper attemps to develop a number of empirical equations which allow prediction of former polygon diameters and patterns.

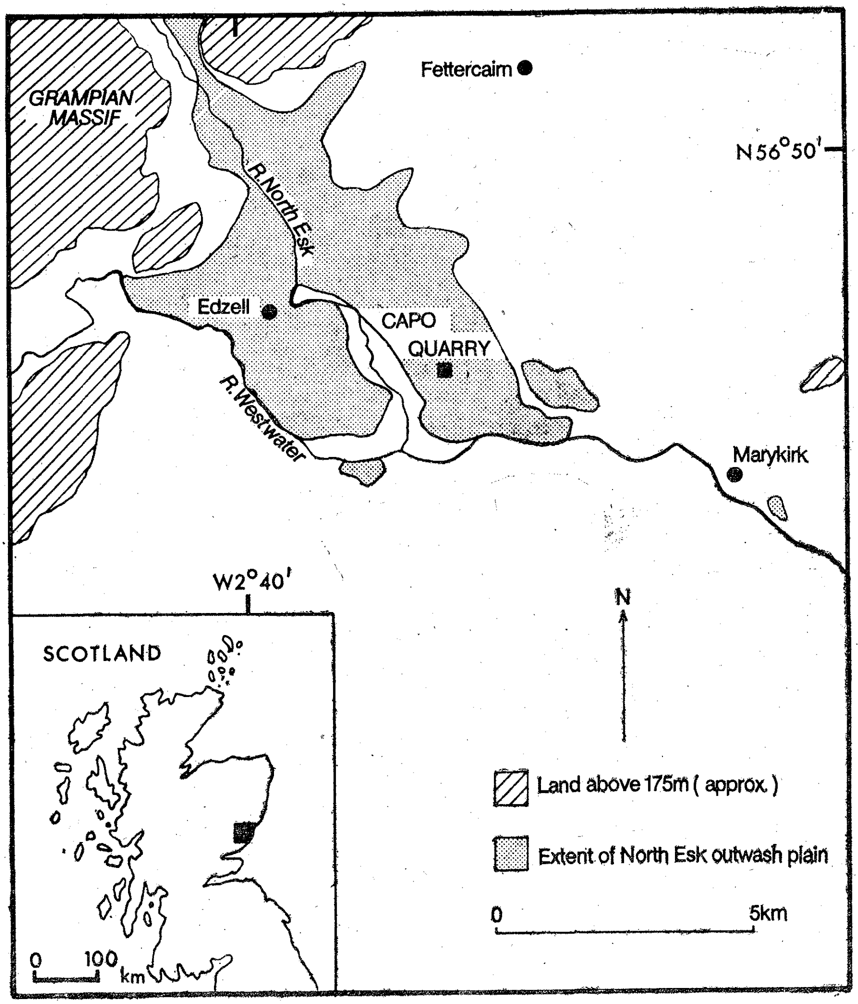

Fig. 1. Location of Capo Quarry, Kincardineshire, north-eastern Scotland

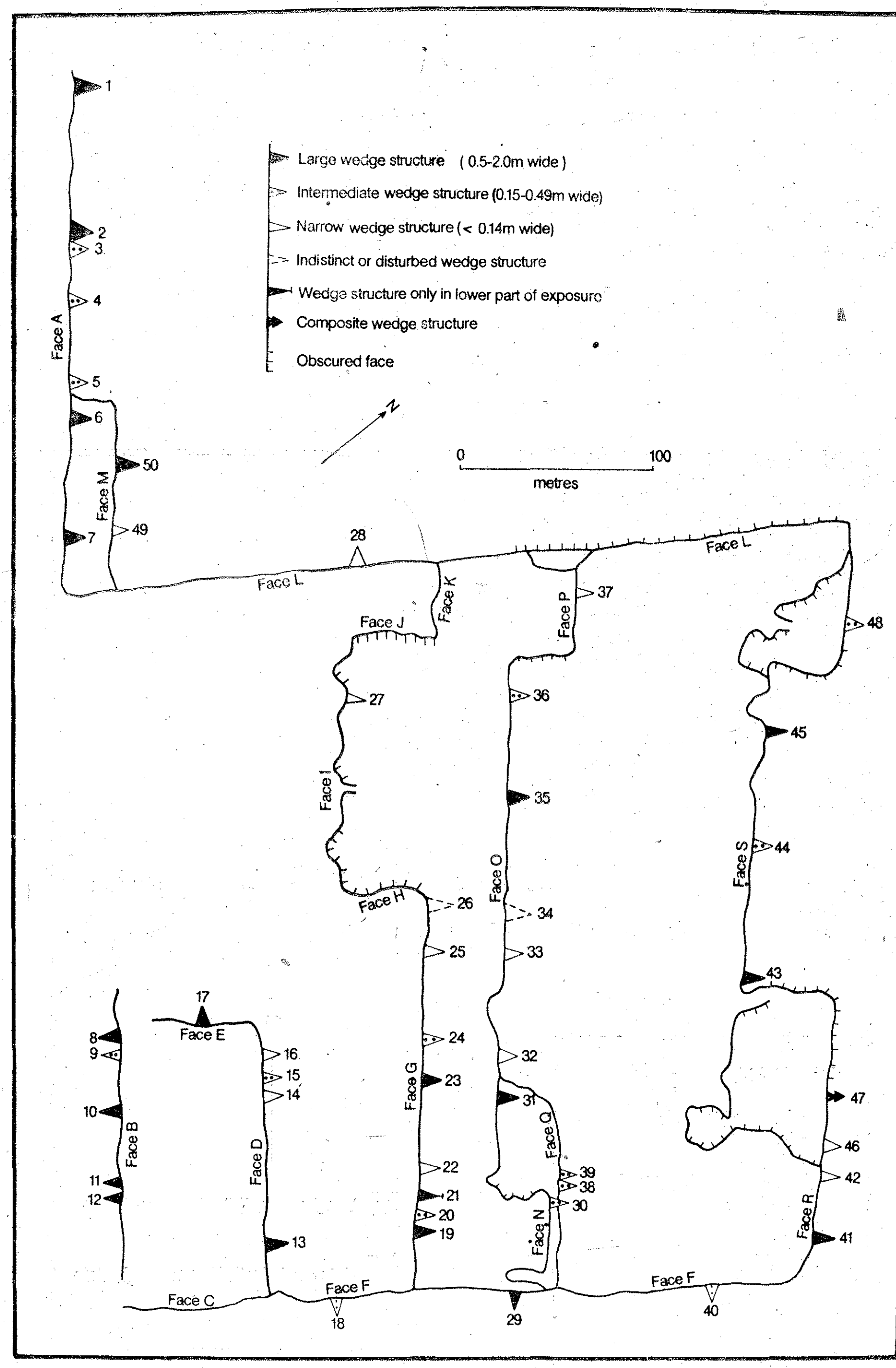

Fig. 2. Location of the frost fissure structures observed during progressive excavation in Capo Quarry

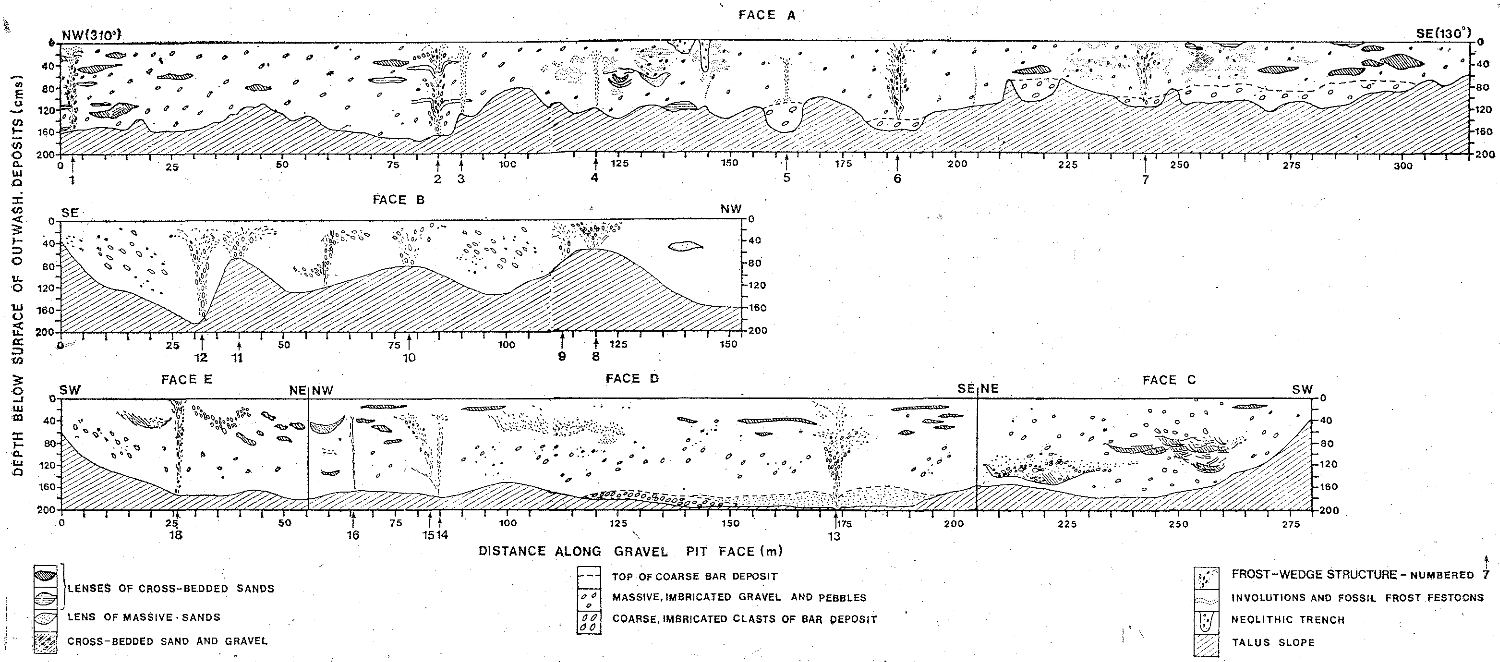

Fig. 3. Exposed sections along faces A to E, Capo Quarry

CAPO QUARRY, KINCARDINESHIRE, EASTERN SCOTLAND

Capo Quarry is situated in the Vale of Strathmore in eastern Scotland (Nat. G.R. No/629671; Fig. 1). The pit is located in coarse outwash sands and gravels deposited as sandur plain by meltwaters issuing from the former North Esk glacier during Late Devensian times (Sissons, 1967, 1974a; Paterson, 1974; Maizels, 1976). Fifty fissure structures were identified over a total length of 1881 m of gravels exposed in 22 vertical faces of the pit at 7 successive stages in pit excavation between August 1973 and September 1980 (Figs 2, 3; Pls 1,2).

DESCRIPTION OF FISSURE STRUCTURES

The fissure structures conspicuously truncate the sediment bedding so that strata and pebbles dip steeply downwards at the wedge margins to merge with the vertically aligned material comprising the wedge infill. Both the infill material and the surrounding sediments comprise coarse bimodal sands and gravels, with mean particle sizes of the gravels averaging between 10.00 mm (SD $= \pm 8.4$) and 6.38 mm (SD $= \pm 7.3$). The infill particles exhibit a distinctive vertical preferred orientation, compared with the imbricate structure of the outwash gravels. Three types of fissure structure have been identified on the basis of structure dimension, morphology and stratigraphical position.

The majority are simple fissure structures originating near the sediment surface. They represent the infilling of a single fissure; the fissure structure appears vertically or obliquely oriented, and exhibits either a rectangular cross--section or becomes narrower with depth. The uppermost zone of sediment deformation associated with these fissure structures lies consistently within 5.0—1.0 m of the sediment surface. In twenty of these structures the maximum width of sediment deformation extends over a lateral distance of up to 2m. These structures normally extend from 0.5 m below the sediment surface to a depth of over 2 m, but their width may either remain constant with depth to form a rectangular cross-section, or taper gradually downwards to form a narrow fissure (Pl. 1). Several fissures exhibit markedly oblique outlines, dipping at angles of 40—60° through the sand and gravel beds.

Sixteen fissures are of intermediate width (0.15—0.49 m wide). They also extend downwards within 0.5 m of the sediment surface and form deep vertical or oblique structures, truncating adjacent sand and gravel beds. An upper wider structure often leads downwards into a narrower oblique or curved fissure, producing a distorted funnel-like fissure outline in cross-section (see also Pl. 1).

Nine fissures are narrow ($\leqslant 0.14$ m wide) and exist as single vein-like fissures extending vertically or obliquely through the outwash deposits. These structures are recognized less by the presence of deformed strata as by the localized vertical alignment of gravel particles and pebbles, and by the local concentrations of silts surrounding the clasts (Pl. 2).

A second type of fissure structure was identified as clearly lying beneath 2.4 m of undeformed sands and gravel, and extending for at least a further 1 m into a basal zone of distorted silts, sands and fine gravels (No 21 on Fig. 2). Adjacent bedded sands were characterized by a number of vertical and oblique faults exhibiting throws of between 3 and 15 mm towards the centre of the fissure.

In addition to the funnel-shaped fissures mentioned above, a distinctive composite "cone-in-cone" fissure structure (JAHN, 1977) was also identified (No. 47 on Fig. 2). The structure extended obliquely into the sands and gravels narrowing from 0.85 m to 0.35 m at a depth of 0.97 m, and then widening out once more to 0.6 m before tapering off to 0.32 m in width at a depth of 1.42 m. At this point, the fissure narrowed off to form a thin vein-like feature curving downwards into basal cobble beds.

Involutions and other fault and trough structures of periglacial origin were also observed in the pit exposures.

ORIGIN OF THE FISSURE STRUCTURES

The fissure structures are believed to have originated as thermal contraction cracks which developed during formation of permafrost. Thawing of the permafrost subsequently led to the fissures being infilled with sands and gravels from adjacent and overlying sediments, and the bedding collapsed inwards to form a series of downturned marginal strata. Some workers, however, claim that relic fissure or wedge structures in which adjacent sediments are downturned rather than upturned into the fissure zone were formed either as frost-induced, mineral-filled thermal contraction cracks (e. g. SVENSSON, 1969) or as non-thermal contraction cracks such as those produced during desiccation, thermokarst erosion or tension release associated with terrace dissection (e. g. JAHN, 1977; GOŹDZIK, 1973; BLACK, 1976).

The fissure structures observed in Capo Quarry are interpreted as relic frost cracks the majority of which are of epigenetic origin, which formed during Younger Dryas times.

The fissures of epigenetic origin are characterized by the conformity of their upper limits, consistently lying at a depth of 0.5—1.0 m (*cf.* BERGERSON and FOLLESTAD, 1971). FITZPATRICK (1956, 1958) claims that this level marks the former permafrost table, a level that is now identified by a „hard pan" or indurated layer of sands and gravels. Indeed, above this level the gravels are clearly involuted, indicating the presence of cryoturbation activity in the former shallow active layer. There is increasing evidence of extensive periglacial activity in eastern Scotland during Younger Dryas times, including a number of relic frost fissure structures (e. g. GALLOWAY, 1961a, 1961b; SISSONS, 1967, 1974a, 1974b; SUGDEN, 1974; CLAPPERTON and SUGDEN, 1977; GRAY and LOWE, 1977). Similar structures have also been described from many other sites in Scotland and their origin has been widely attributed to the development of ground ice-

-wedges within a former permafrost zone (e. g. FitzPatrick, 1956; Common and Galloway, 1959; Rice, 1959; McManus, 1966; McLellan, 1969; Rose, 1975).

The presence of at least one intraformational fissure structure indicates that frost fissuring of permafrost occurred during aggradation of the outwash sediments. In addition, the composite fissure structure described above also suggests that while at least two periods of wedge growth occurred, the lower part of the structure also appears to be intraformational in origin, lying at a depth of about 1.0 m. Finally, some of the larger wedges exhibit a similar width throughout their vertical extent, a feature that may reflect their upward, rather than lateral, growth to keep pace with progressive sedimentation. Structures that are of certain syngenetic origin are hence relatively rare; Galloway (1961a) considered that only 4 out of 100 wedge structures examined in Scotland were of syngenetic origin.

ABSENCE OF SURFACE POLYGON NETWORKS

In the North Esk outwash area no surface evidence of polygonal patterns can be recognized either on the ground or from the available air photographs. The apparent absence of any surface pattern may be accounted for by a number of factors, including both surface vegetation and the time at which the air photos themselves were taken. Capo Quarry lies in an area of open arable and pasture country, interspersed with areas of deciduous woodland and coniferous plantations. Polygons are most likely to show up in areas of spring-sown cereals which exhibit light tones on the air photos, compared with the dark tones of autumn-sown cereals, root crops and pastures (Svensson, 1972, 1976). Svensson (1972, 1973) and others (e. g. Rapp and Annersten, 1969; Friedman *et al.*, 1971; Morgan, 1971; Walters, 1978) have also demonstrated that polygonal ground patterns tend to show up only after a period of hot, dry weather. This creates some degree of "stress" in the ground vegetation, since differences between plant growth along the polygonal boundaries and within the polygon centres are accentuated as a result of contrasts in moisture conditions within the soil environments, thus producing distinctive tonal contrasts on air photos. In the Capo area, however, the particle size characteristics of the wedge infills do not differ significantly from those of the interwedge zones, or polygon centres, and all are very coarse (greater than — 2,5 Θ). In addition, any original surface pattern of ice-wedge polygons may have been destroyed by thermokarst activity (e. g. see Péwé, 1973) or simply by subsequent cryogenic activity or pedogenic processes (e. g. Goździk, 1973).

SPATIAL DISTRIBUTION OF FISSURE STRUCTURES

FIELD MEASUREMENT

The location of each fissure structure exposed along each pit face was mapped by compass traverse, while the distance between individual structures is based on measurements from the centre of each structure. The degree to which the structure is exposed on the pit face will clearly affect the measurements of the dimensions of the structure, with the exposed dimensions increasing from a central cross-section through a diagonal cross-section to a longitudinal cross-section (MACKAY, 1977). In addition, the original wedge size may not necessarily be retained owing to slumping and sediment redistribution during thawing (PISSART, 1970).

MEAN WEDGE SPACING

Mean wedge spacing, MWS, was calculated from the length of those exposed faces which exhibited more than one fissure structure, as:

$$\text{MWS} = \frac{\Sigma \text{L}}{\text{N}_\text{f}} \tag{1}$$

where ΣL = total length of faces and N_f = number of fissure structures. The MWS for Capo Quarry was found to be 36.84 ($\pm$ 26.21 m). This value can be interpreted as representing a "mean linear density" of about 27 fissures per km, a figure that compares closely with 31 present-day ice-wedges per km (i.e. MWS = 32.3 m) that Mackay (1972) considered a common occurrence in areas of continuous permafrost.

LINEAR NEAREST NEIGHBOUR ANALYSIS

The "linear nearest neighbour statistic", LR, was adopted as the most suitable spatial statistical measure of the distribution of fissure structures along a line or linear traverse, where

$$\text{LR} = \frac{\overline{\text{D}}_\text{L}}{0.5\text{L}/(\text{N}_\text{f} - 1)} \tag{2}$$

where

$$\overline{\text{D}}_\text{L} = \frac{\Sigma \text{d}_\text{L}}{\text{N}_\text{f}} \tag{3}$$

D_L is the mean nearest neighbour distance between neighbouring fissure structures along the exposed faces, Σd_L is the sum of nearest neighbour distances for all structures, L is the total length of exposed faces, and $L/(N_f - 1)$ represents an "adjusted linear density" of structures along the selected face, which accommodates the fact that there is a total of $(N_f - 1)$ spaces between all the points on the exposed faces (PINDER, pers. comm.). This statistic, proposed by

PINDER and WITHERICK (1973), allows one to determine how closely the distribution of points along a line approximates to a random distribution, and is based on a modification of the "normal" areal nearest neighbour statistic (e. g. CLARK and EVANS, 1954; BARTON and DAVID, 1956; DACEY, 1960; PEARSON, 1963; KING, 1969). In a random distribution LR = 1.0, while $1.0 < LR < 2.0$ characterizes a regular distribution, and $LR < 1.0$ a clustered distribution of structures along the exposed face. The end of each face may be defined either by the last structure present or by the end of the exposed face. In the latter case, the first and last structures cannot then also be used as points in the calculation of LR. In addition, since the distribution of wedges on each face may not be independent of those on neighbouring or opposite faces, it may be preferable to use those measurements taken from only one of two such faces, unless they are located more than one $\overline{D}_L$ distance apart.

Calculations of the linear distribution of the fissure structures in Capo Quarry produced an LR value of 1.361. This value falls above the upper 95 per cent confidence limit of 1.23 separating significantly random and significantly regular distributions (PINDER and WITHERICK, 1973). Hence, considering all 50 fissures together, they appear to exhibit a significantly regular distribution, i. e. one that exhibits a relatively strong systematic network. This regular component appears to be largely derived from the smaller fissure structures, since the large fissures exhibit an LR value of only 1.17, a highly significant random distribution.

This pattern of fissure distribution in Capo Quarry may reflect a sequential development of fissures, with larger deeper structures forming first, according to random zones of weakness in the permafrost. The narrower structures may have developed at more regular intervals, perhaps during a more extended and more severe period of permafrost formation.

LINEAR AND AREAL MEASURES OF POLYGON PATTERNS

In order to establish the characteristics of former polygonal networks, investigations were directed towards determining whether any predictive relationships exist between known linear distributions of fissure structures and the areal distributions of associated polygonal patterns. Three measures of areal distribution were selected as equivalent to the three linear measures, MSW, $\overline{D}_L$ and LR.

These equivalent areal measures are, respectively, mean polygon diameter, MPD, where

$$\text{MPD} = \frac{\Sigma \text{PD}}{N_p} \tag{4}$$

(where ΣPD = sum of diameters of all polygons cross by transect lines, and N_p = total number of polygons); mean nearest neighbour distance, $\overline{D}_A$, where

$$\overline{D}_A = \frac{\Sigma di}{N_v} \tag{5}$$

(where Σdi = sum of the first nearest neighbour distances of polygon vertices in a given area, and N_v = total number of polygon vertices); and the nearest neighbour index, R, where

$$R = \frac{\overline{D}_A}{\sqrt{0.5\,(A/N_v)}} \tag{6}$$

(where A = area in which polygons occur, km^2).

Comparison of the linear and areal distributions of fissure structures and fissure polygons was based on the analysis of a number of polygon networks

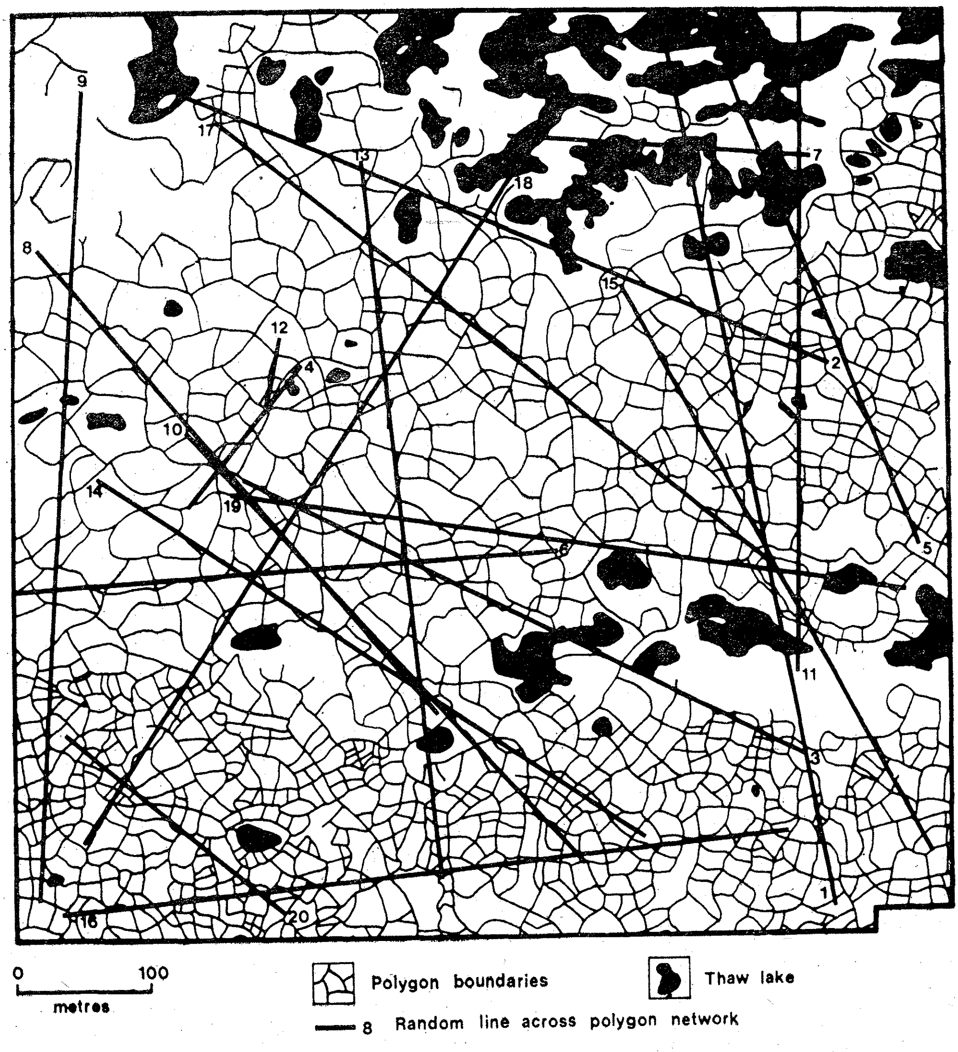

Fig. 4. Pattern of polygons near Barrow, on the coastal plain of Northern Alaska, taken from air photographs 1448-2-165 and 166, 16 July 1964, scale approx. 1 : 3000 (U.S. Army Cold Regions Res. Engr. Lab.). The random transect lines are also indicated (Area 1)

mapped by the author from air photographs or published in the literature. Calculations of MSW, $\overline{D}_L$ and LR were derived from measurements made along a series of random lines extending across each network (see Fig. 4) and taken to simulate possible and independent linear exposures. MPD was calculated from the mean diameter of polygons lying along each of the random lines, while values of $\overline{D}_A$ and R were calculated for the first nearest neighbour polygon vertices within a relatively "homogeneous" network area (see SIBLEY, 1976). Polygon vertices are represented by junction points between adjacent polygons, by points where sharp angular changes in polygon outline occur, or by the termination point of an isolated or single polygon boundary.

DETECTION OF POLYGONAL PATTERNS FROM AIR PHOTOGRAPHS

Air photograph analysis of active and relic ice-wedge polygonal patterns in three areas provide basic pattern information (Tab. I) required to relate linear to areal measures of frost-fissure and polygon distributions.

NORTHERN ALASKA (AREA 1)

Boundaries of ice-wedge polygons are clearly defined on black and white air photographs at a scale of 1 : 3000. The polygon pattern (Fig. 4) is markedly orthogonal, forming a fairly closed network except where polygon centres are depressed to form thermokarstic ponds (e. g. BLACK, 1969). The polygons are mainly 4- and 5-sided (52 per cent and 26 per cent respectively), although some have up to 11 sides, and the sides are often curved. Mean polygon diameter was calculated as 31. 47 $\pm$ 14.63 m (see Tabl. I), with nearest neighbour distances between polygon vertices averaging 7.72 + 4.20 m.

LAHOLM PLAIN, S. W. SWEDEN (AREA 16)

Relic frost fissure polygons were detected from black and white air photographs (scale 1 : 20,000) of the Laholm Plain, an open cultivated area in southwestern Sweden (Fig. 5). Both clearly defined and indistinct polygons were identified, but they are repeatedly interrupted by roads, field boundaries and settlements. Mean polygon diameter was calculated as 53.13 $\pm$ 30.61 m, although the relatively low resolution of the air photographs may have limited the size of polygons that could be detected. Many of the polygon boundaries appearing on the air photographs seem to be far wider than the original fissures, probably the results of thaw runoff and associated erosion, the effects of frost heave, and vegetative growth within the polygon furrows (e. g. see GRUHN and BRYAN, 1969; RAPP and ANNERSTEN, 1969; PISSART, 1970; SVENSSON, 1972, 1973).

Table I

Linear and areal measures of ice-wedge polygon networks

Area No.	Location	Age	Linear measures						Areal measures							Source
			NW	MWS (m)	SD_{MWS}(m)	$\overline{D}_L$(m)	SD_{D_L} (m)	LR	NP	NV	MPD (m)	SD_{PD} (m)	$\overline{D}_A$ (m)	SD_{DA} (m)	R	
1	Northern Alaska	A	480	18.62	4.19	12.35	7.72	1.5589	443	1635	31.47	14.63	7.72	4.20	1.0923	Air photo analysis
2	Domadalshals, Iceland	F, A	150	22.04	5.67	19.57	12.01	1.5320	112	67	39.69	22.56	16.52	2.22	1.4013	FRIEDMAN *et al.*, 1971
3	Kunes, northern Norway	F	63	22.76	5.24	20.16	14.74	1.6350	26	60	44.65	15.50	15.50	7.83	1.1486	MAACK, 1967
4	Batsfjord, northern Norway	F	51	16.13	5.55	16.42	12.95	1.4559	24	70	25.77	8.71	8.21	2.96	1.1820	MAACK, 1967
5	Adamsfjord, northern Norway	F	82	38.83	12.67	36.72	37.20	1.4256	35	111	75.29	40.17	21.90	7.70	1.3846	ÖHRNGREN, 1967
6	Garry Island, N.W.T.	A	77	5.63	1.37	6.33	4.87	1.4189	36	33	16.29	5.03	4.81	2.58	1.2547	MACKAY, 1974
7	Northern Alaska	A	138	27.25	3.83	19.91	12.57	1.3891	90	147	57.41	20.55	14.84	6.02	1.2411	LACHENBRUCH, 1966
8	Northern Alaska	A	273	16.23	2.87	10.67	5.22	1.3303	200	209	24.93	9.62	8.50	2.80	1.3272	LACHENBRUCH, 1966
9	Northern Alaska	A	715	24.37	4.96	17.26	10.55	1.2514	572	612	39.50	19.68	19.52	6.60	1.3968	LACHENBRUCH, 1966
10	Northern Alaska	A	402	16.65	3.08	a) 13.17	7.87	1.2395	314	a) 125	28.10	10.22	a) 11.58	2.87	1.3402	LACHENBRUCH, 1966
						b) 10.34	7.13	1.2000		b) 510			b) 13.34	6.28	1.6055	
11	Northern Alaska	A	266	12.77	1.40	9.36	5.80	1.4290	229	139	22.91	5.61	10.35	2.52	1.4558	LACHENBRUCH, 1966
12	Enontekiö, northern Finland	A?	52	0.78	0.24	0.74	0.50	1.6722	37	62	1.72	0.34	0.51	0.32	1.1092	SEPPÄLÄ, 1966
13	Donnelly Dome, Alaska	F	74	19.24	2.07	19.50	11.86	1.5582	11	25	43.29	12.12	14.00	5.27	1.3840	PÉWÉ *et al.*, 1969
14	Donnelly Dome, Alaska	F	88	20.13	5.31	19.74	15.42	1.5372	23	24	42.45	12.67	18.59	7.47	1.3371	PÉWÉ *et al.*, 1969
15	Northern Greenland	A	237	40.54	5.43	31.24	15.17	1.2694	193	128	69.41	24.30	24.12	7.86	1.3236	SVENSSON, 1962
16	Laholm Plain, southern Sweden	F	281	33.20	11.54	29.09	25.04	1.1825	151	347	53.13	30.61	21.30	8.70	1.2654	Air photo analysis; SVENSSON, 1972, 1973
17	Cambridgeshire, England	F	243	34.85	10.95	24.92	19.51	1.3241	95	74	56.83	24.02	17.13	8.29	1.3098	Air photo analysis

A — active; F — fossil polygons. Linear measures: NW = number of wedges or polygon boundaries crossing transect lines; MWS = mean wedge spacing; SD_{MWS} = standard deviation of mean wedge spacing; $\overline{D}_L$ = mean nearest neighbour distance between wedges or polygon boundaries along random transect lines; SD_{DL} = standard deviation of D_L distances; LR = linear nearest neighbour index

Areal measures: NP = number of polygons crossed by transect lines; NV = number of polygon vertices within homogeneous polygon area; MPD = mean polygon diameter; SD_{PD} = standard deviation of polygon diameter; $\overline{D}_A$ = mean nearest neighbour distance between polygon vertices; SD_{DA} = standard deviation of D_A distances; R = areal nearest neighbour index

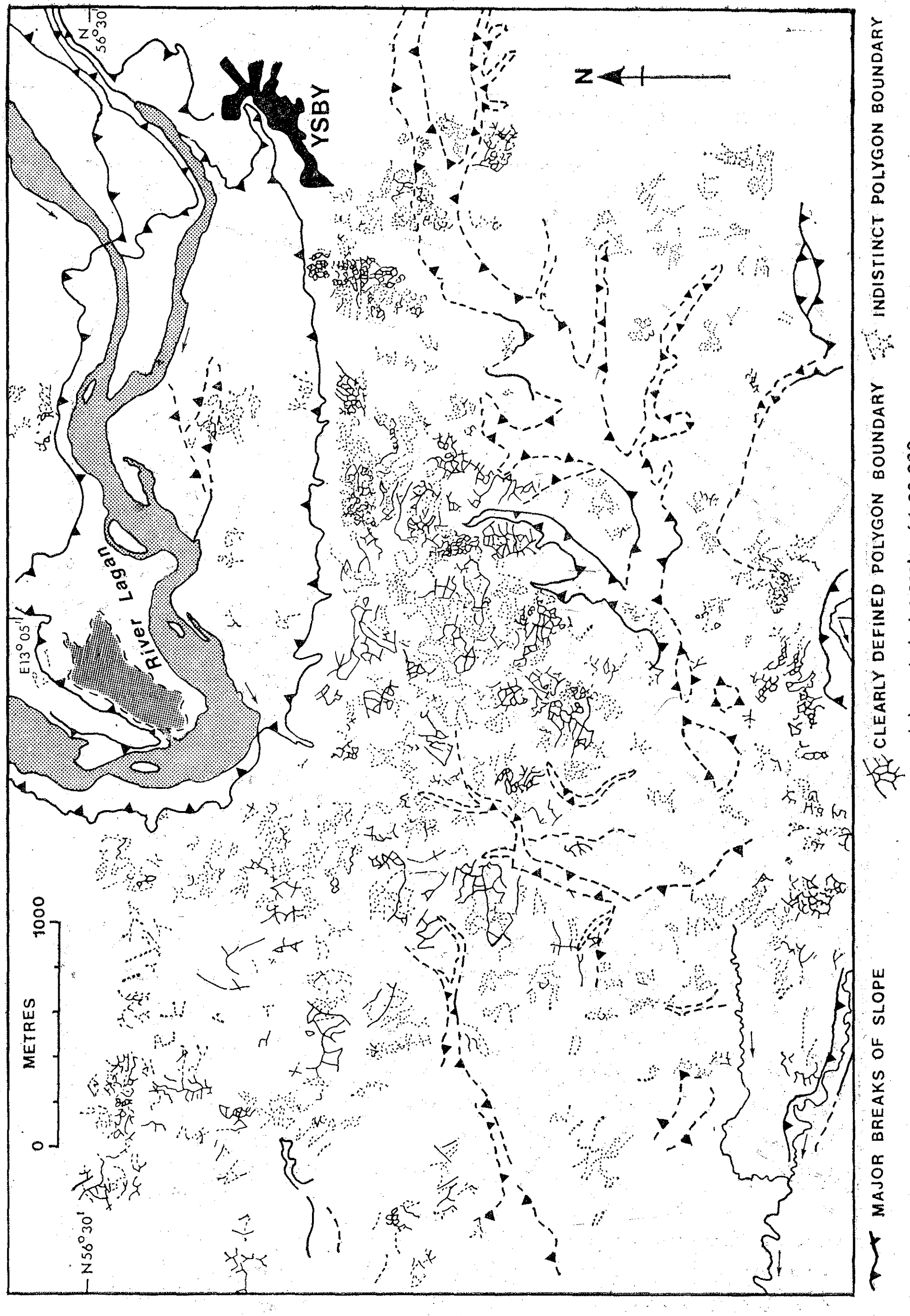

Fig. 5. Interpretation of fossil frost wedge polygon networks from air photographs of the Laholm Plain, Southern Sweden (Area 16). Air photographs Na 47-57-34 (022) and 47-57-35 (021), Statens Lantmäteriverk

CAMBRIDGESHIRE, EASTERN ENGLAND (AREA 17)

A network of Late Devensian relic frost-fissure polygons was mapped from black and white air photographs (scale 1 : 7,500) of a cultivated area in Cambridgeshire, eastern England (Nat. G. R. 135/3877; Fig. 6). Many of the polygons

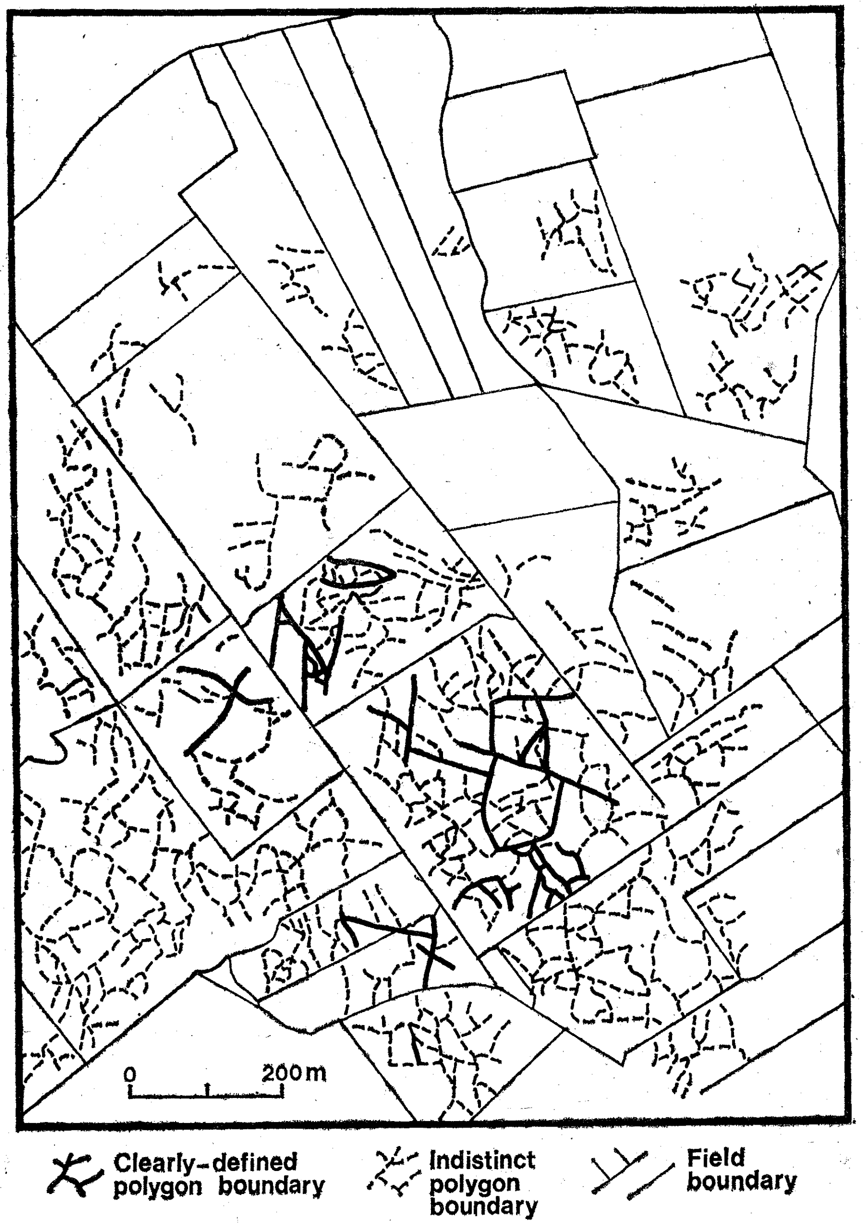

Fig. 6. Devensian polygon network in Cambridgeshire, England (Nat. Grid Ref. 143) 53852767; 0°02′ E, 52°22′ N) based on analysis of air photographs (Ordnance Survey, 70-210/146 and 147; 4th June 1970), scale 1 : 7500

are indistinct features, while a number of polygons are either incomplete, or terminate at isolated or unattached points (see also MAACK, 1967). As on the Laholm Plain, mean polygon diameter is relatively large (MPD = 56.83 m) with a wide range of polygon sizes present ($SD_{PD} = \pm$ 24.02 m). The polygons also exhibit a range of number of sides, the sides often being slightly curved.

OTHER AREAS

Analysis of the linear and areal measures was extended to fourteen other polygonal patterns, both active and relic, from different parts of the northern hemisphere, and published in the literature as maps, plans or air photographs (see Tab. I).

PREDICTION OF FORMER POLYGONAL PATTERNS

PREDICTING MEAN POLYGON DIAMETER

A significant positive linear correlation ($r = +0.96$, $\alpha = 0.001$) was found to exist between mean wedge spacing, MWS, and mean polygon diameter, MPD, despite the enormous variation in pattern types present, such that

(7) $$\text{MPD} = 2.74 + 1.69\ \text{MWS}$$

This close correlation is to be expected since polygon size should, on average, be determined by the distance between polygon boundaries, or fissure structures, regardless of the orientation of the random lines in relation to the polygon network. The range of polygon sizes may also be estimated from the simple equation

(8) $$SD_{PD} = -2.60 + 0.48\ \text{MPD},$$

where SD_{PD} represents the standard deviation of polygonal diameters (with $r = +0.90$, $\alpha = 0.001$).

These empirically derived equations have been used to estimate the diameters of former frost-fissure polygons in the area of Capo Quarry, such that MPD = = 65.00 ± 28.60 m. These polygon sizes would resemble those recorded by SVENSSON (1962) in Northern Greenland, where MPD averaged 69.41 ± 24.30 m (Tab. I, Area 15). GOŹDZIK (1964) also attempted to estimate polygonal diameter from the spacing of wedge structures, based on a 20 km long aqueduct in Poland. According to equation (7), however, GOŹDZIK's calculations may actually have underestimated former MPD_S by up to 70 per cent.

PREDICTING MEAN NEAREST NEIGHBOUR DISTANCE BETWEEN POLYGON VERTICES

The mean distance between nearest neighbour polygon vertices in each "homogeneous" polygon network, $\overline{D}_A$, was found to be significantly correlated ($r = +0.90$, $\alpha = 0.001$) with the mean distances between the nearest neighbour polygon boundaries along the random line $\overline{D}_L$, (Fig. 7) such that

(9) $$\overline{D}_A = 2.77 + 0.63\ \overline{D}_L$$

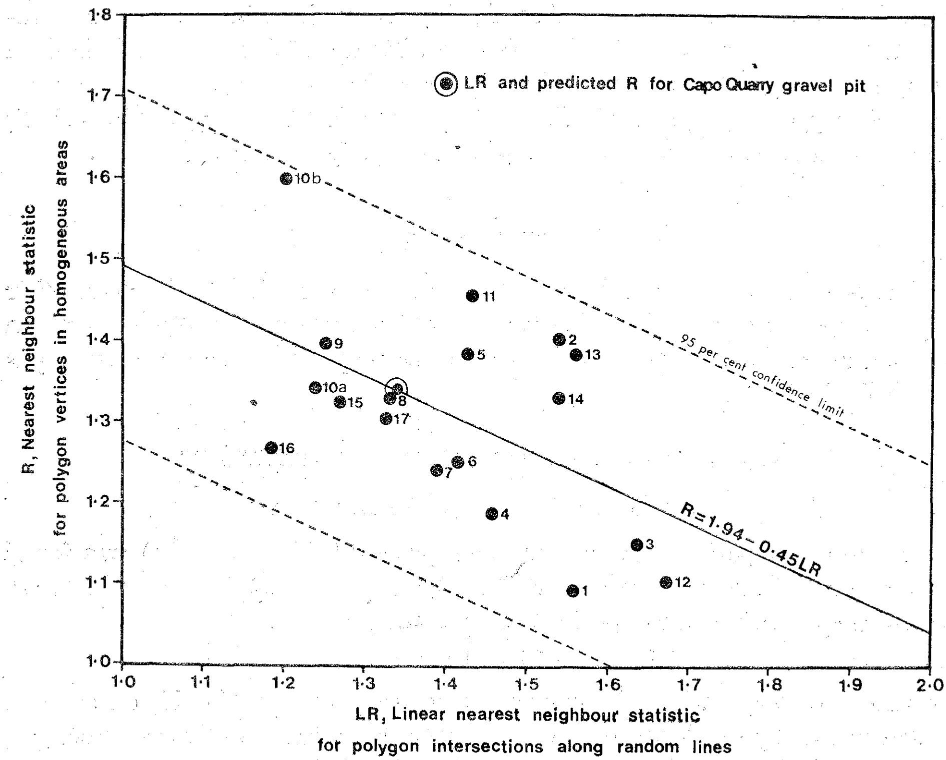

Fig. 7. Relationships between „linear" and „areal" nearest neighbour distances for 17 polygon networks

Table II

Observed and predicted linear and areal measures of polygon pattern in Capo Quarry

Linear measures					Areal measures			
Measure	Observed value $\bar{x}$	S.D.	Value measured from simulation (Fig. 10)		Measure	Value predicted from empirical relations (equations 7a—10) $\bar{x}$	S.D.	Value measured from simulation (Fig. 10)
MWS (m)	36.84	26.21	31.82	16.34	MPD (m)	65.00	28.60	65.00*
$\overline{D}_L$ (m)	29.77		19.75		$\overline{D}_A$ (m)	21.53	5.50	24.50
LR	1.36		1.20		R	1.31	0.05	1.27

* Simulated MPD value set to match scale of output

This is a useful relationship in that it allows one to estimate from fissure structure spacing along a linear exposure, the probable areal distribution of polygon vertices, and hence the probable type (or range of possible types) of former polygonal network. The calculated $\overline{D}_A$ value for Capo Quarry is 21.53 m representing a $\overline{D}_L$ value of 29.77 m (Tab. II).

PREDICTING POLYGON "PATTERN"

A fairly high inverse correlation ($r = -0.53$, $\alpha = 0.005$) was found between the value of the linear nearest neighbour statistic of fissure distributions, LR, and the areal nearest neighbour statistic of polygon vertices, R (Fig. 8), such that

$$R = 1.94 - 0.45\ LR \tag{10}$$

Bearing in mind the problems associated with the interpretation of R values in terms of polygon "pattern" (see discussions in EBDON, 1976; VINCENT, 1976; PINDER, 1978), one can estimate from equation (10) the possible type of polygon network that might have existed in the Capo Quarry area. A predicted R value of 1.31 ($\pm$ 0.05) for Capo Quarry suggests a fairly regular polygonal pattern with a distribution of polygon vertices similar to that of, for example, Area 10a in northern Alaska (Tab. I). However, the Capo Quarry fissure polygons would have been larger with an MPD of 65 m compared with only 28 m in the mapped area of northern Alaska.

SIMULATING FORMER POLYGONAL PATTERNS

The distribution of nearest neighbour distances within a given area was used to generate a series of probability distributions of vertices and of polygon sides

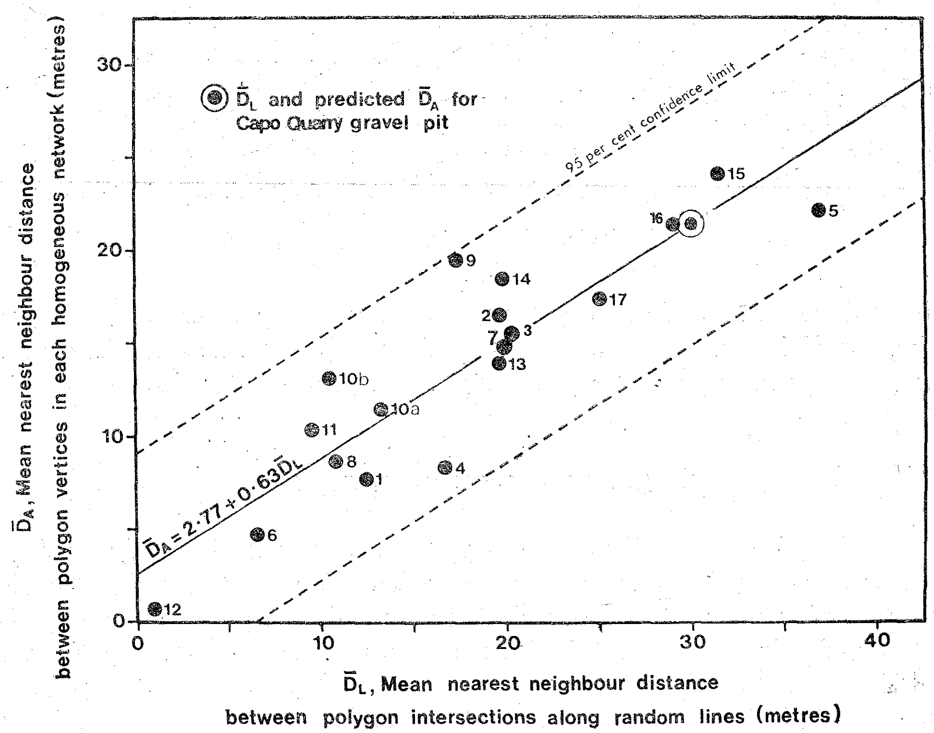

Fig. 8. Relationships between „linear" and „areal" nearest neighbour indices for 17 polygon networks

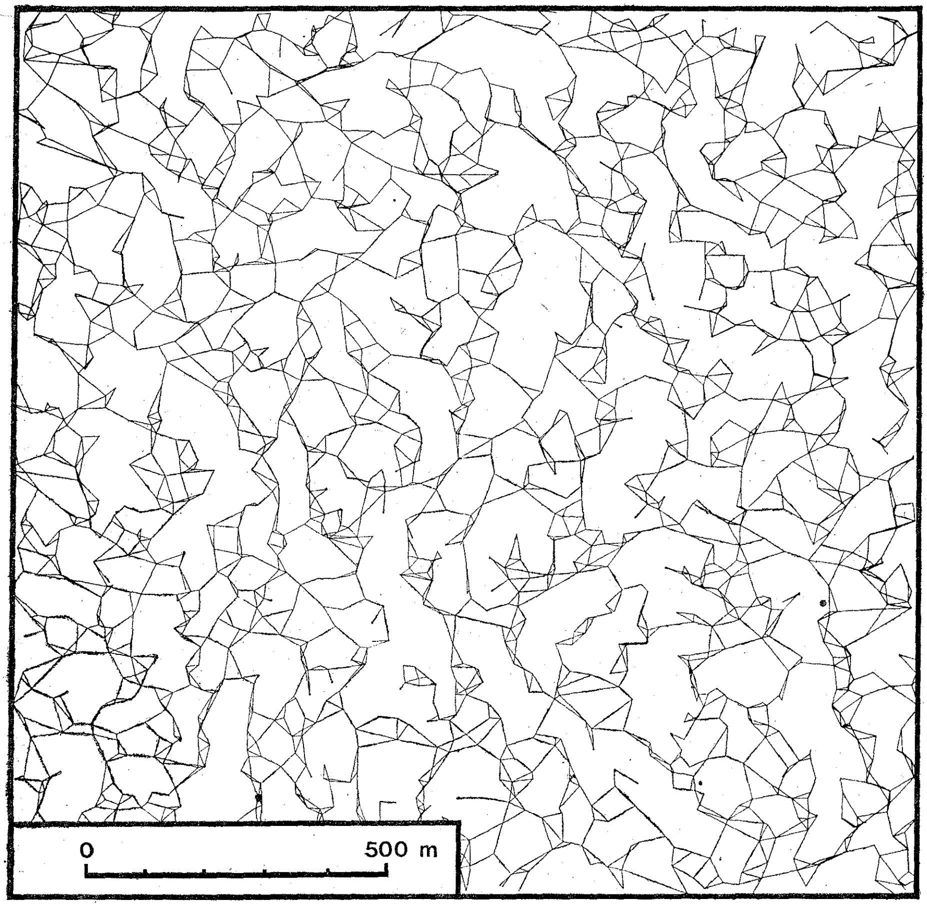

Fig. 9. Simulation of a random polygonal pattern

joining these vertices. Two computer simulation procedures were adopted, both using topological principles and based on the polygon vertex as the basic input variable, representing the end-point or junction point of each fissure.

RANDOM POLYGON DISTRIBUTION

A series of randomly distributed polygons was produced in the first simulation procedure by introducing simple operational constraints defining the distribution of vertices (here, random distribution of 2000 points was used), the number of polygon sides meeting at each vertex (here, a maximum of 5 was specified), and the minimum angle between adjacent sides (here, Θ varied between 30° and 90°), where the number of sides meeting at each vertex is inversely related to the number of sides of each polygon.

Several graphics problems were encountered, however, for the polygon

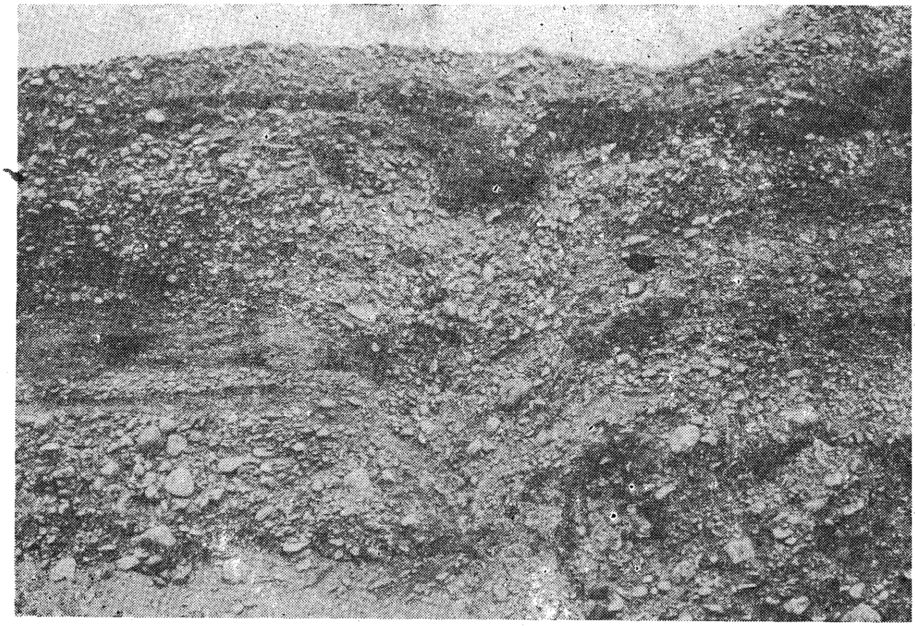

Pl. 1. Large funnel-shaped fissure structure (No. 43) in Capo Quarry gravel pit

The fissure structure extends over a maximum width of ca 1.7 m in the upper part of the section, but narrows markedly at a depth of 1.3 m to form a structure only ca. 0.25 m wide

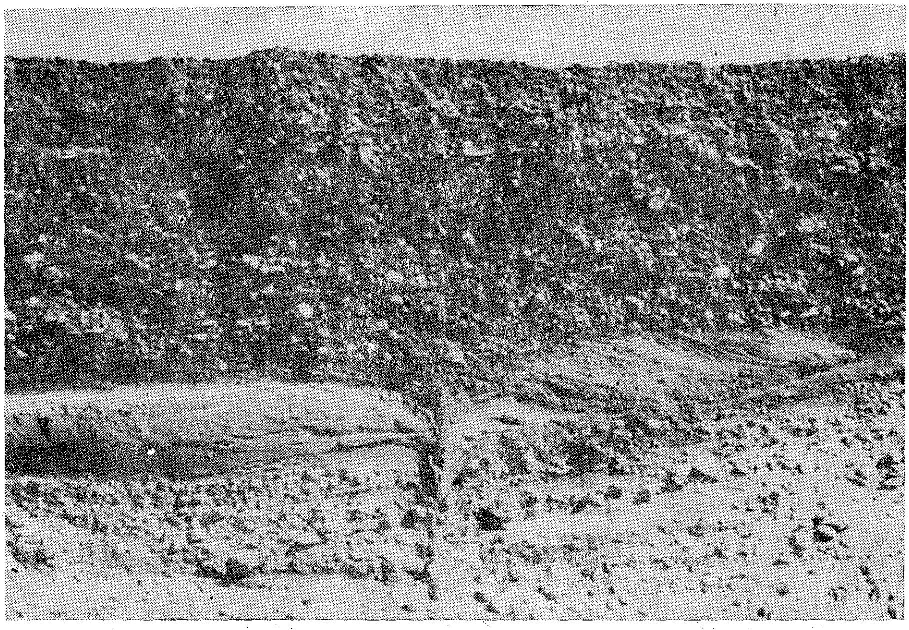

Pl. 2. Narrow fissure structure (No. 33) in Capo Quarry gravel pit

Maximum width is only 0.12 m. Although the structure is clearly detectable in the lower sands and gravels, the coarse upper pebble beds appear to have masked its extension at higher levels in the section boundaries could only be plotted as straight lines, and these tended to cross, or to be almost superimposed on, one another. The resulting polygon patterns therefore tended to be dominated particularly by 3-sided figures (Fig. 9).

REGULAR POLYGON DISTRIBUTION

A more systematic distribution of polygons was created from an initial regular grid of vertices; each polygon vertex in the simulation was then located at a random distance and direction from the original vertex position. The resulting pat-

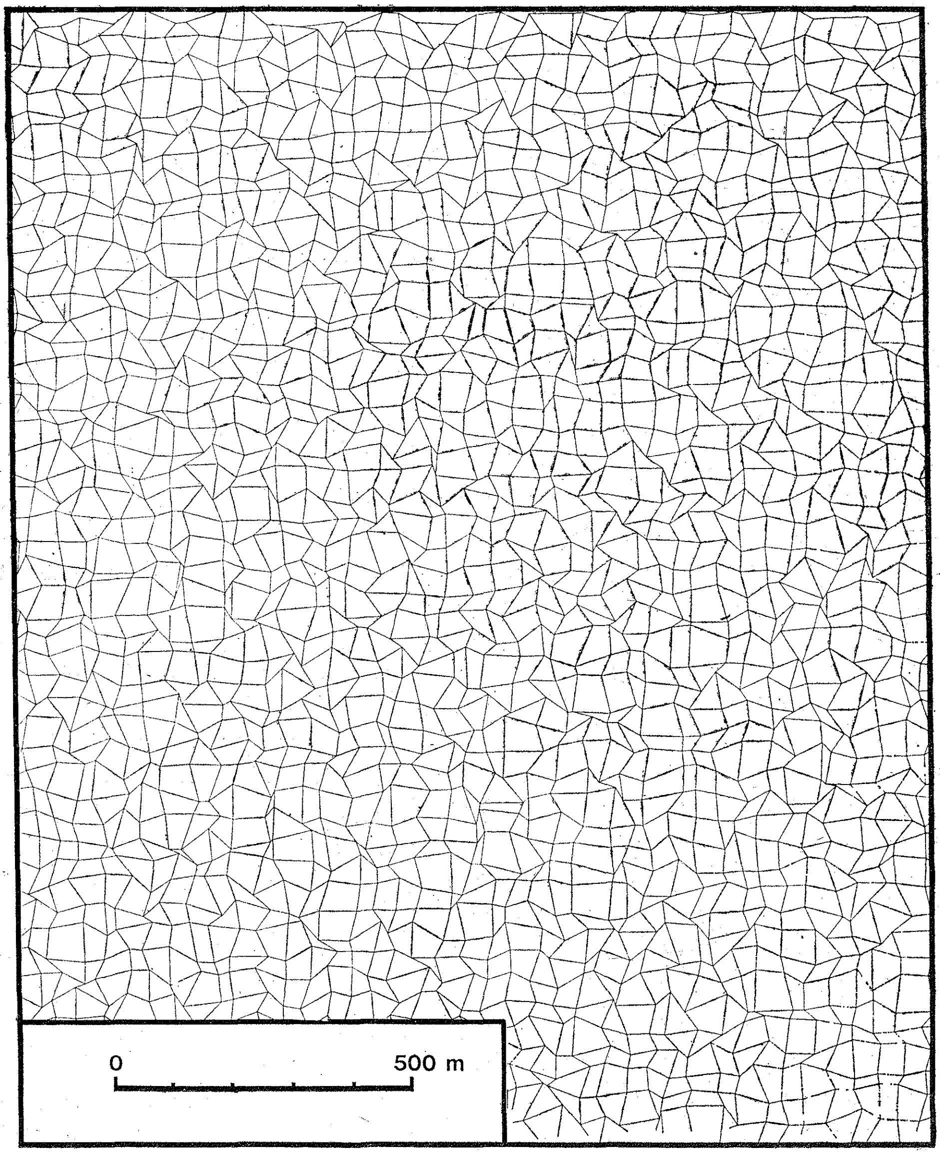

Fig. 10. Simulation of a systematic polygonal pattern

terns (e.g. Fig. 10) possess a predominance of 4-sided polygons, a relatively small range of polygon diameters, and a series of orthogonally oriented polygon boundaries.

The polygonal network illustrated in Fig. 10 is considered to represent one likely form of the fissure network exposed in the Capo Quarry. It exhibits a significantly systematic pattern in the distribution of polygon vertices, as demanded by the predicted R value of 1.31. The values of MPD, $\overline{D}_A$ and R calculated for this simulated polygon pattern correspond closely with those estimated for Capo Quarry (Tab. II).

CONCLUSION

The presence of syngenetic ice-wedge fissures in the Capo Quarry sediments suggests that permafrost may have been present towards the close of the Late Devensian. However, the majority of the wedge structures are believed to represent ice-wedge fissures that formed during the Younger Dryas period. Sissons (1974b) and Lowe and Walker (1977) calculated that mean July temperatures in the southeast Grampians during Younger Dryas times were about 7°—9°C lower than at present, i.e. averaging about 5—6°C. However, if mean annual temperatures (at present about 8°C) were also reduced by this amount, they would average only about −1°C, a value that appears far too high for the development of continuous permafrost; a minimum mean annual air temperature of −6°C to −8°C appears to be necessary (Péwé, 1966) while in coarse gravels even lower temperatures may be required. Hence, it appears that mean annual temperatures must have fallen some 16°C below present temperatures to reach −8°C, in turn resulting in a far more extreme annual temperature range (from +5°C to −22°C) of 27°C.

The existence of such low temperature conditions is supported by the measurements of fissure spacing and predicted polygon dimensions in Capo Quarry when compared with comparable patterns in areas of contemporary permafrost. Mean wedge spacing in Capo Quarry was found to be similar to that considered by Mackay (1972, 1974) to be common at Garry Island, N.W.T., where a mean annual ground surface temperature of −7°C to −10°C has been recorded, and where permafrost is over 360 m thick. The measurements of fissure patterns at Capo Quarry and their interpretation as relic ice-wedge fissures suggests that mean annual air temperatures, and particularly winter temperatures, in eastern Scotland during Younger Dryas times, were considerably lower than hitherto realised.

ACKNOWLEDGEMENTS

The author would like to thank Dr. R.B.G. Williams, University of Sussex, for his many helpful comments on the paper, and Mr. D. Waddell, Bedford College Computer Unit, for his assistance in writing the computer programs.

The author is also grateful to Dr. D. PINDER, University of Southampton, and Dr. S. EMBLETON, King's College, University of London, for their useful comments, and to Dr. H. SVENSSON, University of Copenhagen, for interesting discussions in the field.

References

BARTON, E. D. and DAVID, F. N., 1956 — Tests for randomness of points on a line. *Biometrika,* 43; p. 104—112.

BERGERSON, O. F. and FOLLESTAD, B. A., 1971 — Evidence of fossil ice wedges in Early Weichselian deposits at Foss-Eikjeland, Jaeren, south-west Norway. *Norsk Geogr. Tidsskr.*, 25; p. 39—45.

BLACK, R. F., 1969 — Climatically significant fossil periglacial phenomena in north central United States. *Biuletyn Peryglacjalny*, 20; p. 225—238.

BLACK, R. F., 1976 — Periglacial features indicative of permafrost: ice and soil wedges. *Quatern. Res.*, 6; p. 3—26.

CLAPPERTON, C. M. and SUGDEN, D. E., 1977 — The Late Devensian glaciation of north-east Scotland. *in*: Studies in the Scottish Lateglacial environment. Pergamon Press (Eds.: J. M. GRAY and J. J. LOWE); p. 1—13.

CLARK, P. J. and EVANS, F. C., 1954 — Distance to nearest neighbour as a measure of spatial relationships in population. *Ecology*, 35; p. 445—453.

COMMON, R. and GALLOWAY, R. W., 1958 — Ice wedges in Midlothian: a note. *Scott. Geogr. Mag.*, 74; p. 44—46.

CORTE, A. and HIGASHI, A., 1964 — Experimental research on desiccation cracks in soil. *U.S. Army Material Command, Cold Reg. Res. Eng. Lab., Hanover, New Hampshire, Res. Report* 66; 72 p.

DACEY, M. F., 1960 — The spacing of river towns. *Ann. Assoc. Amer. Geogr.*, 50; p. 59—61.

DOSTOVALOV, B. N. and POPOV, A. I., 1966 — Polygonal systems of ice wedges and conditions of their development. *in*: *Proc. 1st Internat. Permafrost Conf., Nat. Acad. Sci., Nat. Res. Counc.*, Publ. 1287; p. 63—71.

DYLIK, J., 1966 — Problems of ice-wedge structures and frost-fissure polygons. *Biuletyn Peryglacjalny*, no. 15; p. 241—291.

EBDON, D., 1976 — On the underestimation inherent in the commonly used formulae. *Area*, 8; p. 165—169.

FITZPATRICK, E. A., 1956 — Progress report on the observations of periglacial phenomena in the British Isles. *Biuletyn Peryglacjalny*, 4; p. 99—115.

FITZPATRICK, E. A., 1958 — An introduction to the periglacial geomorphology of Scotland. *Scott. Geogr. Mag.*, 74; p. 28—36.

FRIEDMAN, J. D., JOHANSSON, C. E., OSKARSSON, N., SVENSSON, H., THORARINSSON, S. and WILLIAMS, R. S., JR., 1971 — Observations on Icelandic polygon surfaces and palsa areas. Photo-interpretation and field studies. *Geogr. Annaler*, 53; p. 115—145.

GALLOWAY, R. W., 1961a — Ice wedges and involutions in Scotland. *Biuletyn Peryglacjalny*, no. 10; p. 169—193.

GALLOWAY, R. W., 1961b — Periglacial phenomena in Scotland. *Geogr. Annaler*, 43; p. 348—353.

GOŹDZIK, J. S., 1964 — L' étude de la répartition topographique des structures périglaciaires. *Biuletyn Peryglacjalny*, 14; p. 217—249.

GOŹDZIK, J., 1973 — Geneza i pozycja stratygraficzna struktur peryglacjalnych w środkowej Polsce (Summary: Origin and stratigraphical position of periglacial structures in Middle Poland). *Acta. Geogr. Lodziensia*, 31; 117 p.

GRAY, J. M. and LOWE, J. J., 1977 — The Scottish Lateglacial environment: A synthesis. *in*: Studies in the Scottish Lateglacial environment. Pergamon Press (Eds.: J. M. GREY and J. J. LOWE); p. 163—181.

GRUHN, R. and BRYAN, A. L., 1969 — Fossil ice wedge polygons in southeast Essex, England. *in*: The periglacial environment. Past and present. McGill-Queen's Univ. Press, Montreal, (Ed., T. L. PÉWÉ); p. 351—363.

JAHN, A., 1977 — Classification of the Pleistocene frost- and ice-wedge structures. *Biuletyn Peryglacjalny*, 27; p. 175—177.

KING, L. J., 1969 — Statistical analysis in geography. Prentice Hall Inc.; 288 p.

LACHENBRUCH, A. H., 1962 — Mechanics of thermal contraction cracks and ice-wedge polygons in permafrost. *U.S. Geol. Surv., Spec. Paper*, 70; 69 p.

LACHENBRUCH, A. H., 1966 — Contraction theory of ice-wedge polygons: a qualitative discussion. *In : Proc. 1st Internat. Permafrost Conf.*, 1965, *Nat. Acad. Sci., Nat. Res. Counc.*, Publ. 1287; p. 63—71.

LOWE, J. J. and WALKER, M. J. C., 1977 — The reconstruction of the Lateglacial environment in the southern and eastern Grampian Highlands. *in*: Studies in the Scottish Lateglacial environment. Pergamon Press (Eds.: J. M. GRAY and J. J. LOWE); p. 101—118.

MAACK, A., 1967 — Fossil ice-wedge polygons in the Kunes and Båtsfjord areas. *Lund Stud. in Geogr.*, ser. A, 40; p. 41—57.

MACKAY, J. R., 1972 — The world of underground ice. *Ann. Assoc. Amer. Geogr.*, 62; p. 1—22.

MACKAY, J. R., 1974 — Ice-wedge cracks, Garry Island, North West Territories. *Canad. Jour. Earth Sci.*, 11; p. 1366—1386.

MACKAY, J. R., 1977 — The width of ice-wedges. *Geol. Survey of Canada*, Paper 77—1A; p. 43—44.

MAIZELS, J. K., 1976 — A comparison of present-day and Pleistocene proglacial environments, with particular reference to morphology and sedimentology. Unpub. Ph. D. thesis, Univ. of London; 675 p.

MAIZELS, J. K., 1981 — Freeze-thaw experiments in the simulation of sediment cracking patterns Occasional Paper No. 13, Dept. Geogr., Bedford Coll., Univ. London; 34 p.

MCLELLAN, A. G., 1969 — The last glaciation and deglaciation of central Lanarkshire. *Scott. Jour. Geol.*, 5; p. 248—268.

MCMANUS, J., 1966 — An ice-wedge and associated phenomena in the Lower Limestone Series of Fife. *Scott. Jour. Geol.*, 2; p. 259—264.

MORGAN, A. V., 1971 — Polygonal patterned ground of Late Weichselian age in the area north west of Wolverhampton, England. *Geogr. Annaler*, 53; p. 146—156.

ÖHRNGREN, S., 1967 — Polygon fields on the Lakesfjord, Finnmark. *Lund Stud. in Geogr.*, ser. A, 40; p. 58—67.

PATERSON, I. B., 1974 — The supposed Perth Readvance in the Perth district. *Scott. Jour. Geol.*, 10; p. 53—66.

PEARSON, E. S., 1963 — Comparison of tests for randomness of points on a line. *Biometrika*, 50; p. 315—325.

PÉWÉ, T. L., 1966 — Paleoclimatic significance of fossil ice-wedges. *Biuletyn Peryglacjalny*, 15; p. 65—73.

PÉWÉ, T. L., 1973 — Ice wedge casts and past permafrost distribution in North America. *Geoforum*, 15; p. 15—26.

PÉWÉ, T. L., CHURCH, R. E. and ANDERSON, M. J., 1969 — Origin and paleoclimatic significance of large-scale patterned ground in the Donnelly Dome Area, Alaska. *Geol. Soc. Amer., Spec. Paper* 103; 87 p.

PINDER, D. A., 1978 — The elimination of under-estimation in nearest-neighbour analysis. Disc. Paper No. 1, Dept. Geogr., Univ. Southampton; 18 p.

PINDER, D. A. and WITHERICK, M. E., 1973 — Nearest-neighbour analysis of linear point patterns. *Tijdschr. v. Econ. en Soc. Geogr.*, 64; p. 160—163.

PISSART, A., 1968 — Les polygones de fente de gel de l'Ile Prince Patrick (Arctique Canadien — — 76° lat. N). *Biuletyn Peryglacjalny*, 17; p. 171—180.

PISSART, A., 1970 — Les phénomènes physiques éssentiels liés au gel, les structures périglaciaires qui en resultent et leur signification climatique. *Ann. Soc. Geol. Belg.*, 93; p. 7—49.

RAPP, A. and ANNERSTEN, L., 1969 — Permafrost and tundra polygons in northern Sweden. *in*: The periglacial environment. Past and present. McGill-Queen's Univ. Press, Montreal (Ed T. L. PÉWÉ); p. 65—91.

RICE, R. J., 1959 — A frost wedge in Angus. *Scott. Geogr. Mag.*, 75; p. 50—51.

ROSE, J., 1975 — Raised beach gravels and ice wedge casts at Old Kilpatrick, near Glasgow. *Scott. Jour. Geol.*, 11; p. 15—21.

SEPPÄLÄ, M., 1966 — Recent ice wedge polygons in eastern Enontekiö, northernmost Finland. *Publ. Inst. Geogr. Univ. Turku*, 42; p. 273—287.

SIBLEY, D., 1976 — On pattern and dispersion. *Area*, 8; p. 163—165.

SISSONS, J. B., 1967 — Glacial stages and radiocarbon dates in Scotland. *Scott. Jour. Geol.*, 3; p. 375—381.

SISSONS, J. B., 1974a — Glacial readvances in Scotland. *in*: Problems of the deglaciation of Scotland. *Jour. St. Andrews Geogr., Spec. Publ.*, 1; p. 5—15.

SISSONS, J. B., 1974b — A Late-glacial ice cap in the central Grampians, Scotland. *Inst. Brit. Geogr. Trans.*, 62; p. 95—114.

SUGDEN, D. E., 1974 — Deglaciation of the Cairngorms and its wider implications. *in*: Problems of the deglaciation of Scotland. *Jour. St. Andrews Geogr., Spec. Publ.*, 1; p. 17—28.

SVENSSON, H., 1962 — Tundra polygons. Photographic interpretation and field studies in north-Norwegian polygon areas. *Norges Geol. Unders.*, 223; p. 298—327.

SVENSSON, H., 1969 — Open fissures in a polygonal net on the Norwegian arctic coast. *Biuletyn Peryglacjalny*, 19; p. 389—398.

SVENSSON, H., 1972 — The use of stress situations in vegetation for detecting ground conditions on aerial photographs. *Photogrammetria*, 28; p. 75—87.

SVENSSON, H., 1973 — Distribution and chronology of relic polygon patterns on the Laholm Plain, the Swedish west coast. *Geogr. Annaler*, 55; p. 159—175.

SVENSSON, H., 1976 — Relic ice wedge polygons revealed on aerial photographs from Kaltenkirchen, northern Germany. *Geogr. Tidsskr.*, 75; p. 8—12.

VINCENT, P., 1976 — The general case: how not to measure spatial point patterns. *Area*, 8; p. 161—163.

WALTERS, J. C., 1978 — Polygonal patterned ground in central New Jersey. *Quatern. Res.*, 10; p. 42—54.

Manuscript received: September, 1981